GFZ

Helmholtz-Zentrum
POTSDAM

Originally published as:

Activity concentrations of [238]U and [226]Ra in two European black shales and their experimentally-derived leachates

Franziska D.H. Wilke[1]*, Georg Schettler[1], Andrea Vieth-Hillebrand[1], Michael Kühn[1,2], Heike Rothe[1]

[1]GFZ German Research Centre for Geosciences, Telegrafenberg, 14473 Potsdam, Germany

[2]University of Potsdam, Department of Earth and Environmental Sciences, Karl-Liebknecht Str. 24-25, 14467 Potsdam, Germany

Abstract

The production of gas from unconventional resources became an important position in the world energy economics. In 2012, the European Commission's Joint Research Centre estimate 16 trillion cubic meters (Tcm) of technically recoverable shale gas in Europe. Taking into account that the exploitation of unconventional gas can be accompanied by serious health risks due to the release of toxic chemical components and natural occurring radionuclides into the return flow water and their near-surface accumulation in secondary precipitates, we investigated the release of U, Th and Ra from black shales by interaction with drilling fluids containing additives that are commonly employed for shale gas exploitation.

We performed leaching tests at elevated temperatures and pressures with an Alum black shale from Bornholm, Denmark and a Posidonia black shale from Lower Saxony, Germany. The Alum shale is a carbonate free black shale with pyrite and barite, containing 74.4 µg/g U. The Posidonia shales is a calcareous shale with pyrite but without detectable amounts of barite containing 3.6 µg/g U.

Pyrite oxidized during the tests forming sulfuric acid which lowered the pH on values between 2-3 of the extraction fluid from the Alum shale favoring a release of U from the Alum shale to the fluid during the short-term and in the beginning of the long-term experiments. The activity concentration of [238]U is as high as 23.9 mBq/ml in the fluid for those experiments. The release of U and Th into the fluid is almost independent of pressure. The amount of uranium in the European shales is similar to that of the Marcellus Shale in the United States but the daughter product of [238]U, the [226]Ra activity concentrations in the experimentally derived leachates from the European shales are quite low in comparison to that found in industrially derived flowback fluids from the Marcellus shale. This difference could mainly be due to missing Cl in the reaction fluid used in our experiments and a lower fluid to solid ratio in the industrial plays than in the experiments due to subsequent fracking and minute cracks from which Ra can easily be released.

Key words: unconventional gas production, black shales, flowback, radioactivity, NOR, batch experiments

Activity concentrations of ^{238}U and ^{226}Ra in two European black shales and their experimentally-derived leachates

Abstract

The production of gas from unconventional resources became an important position in the world energy economics. In 2012, the European Commission's Joint Research Centre estimate 16 trillion cubic meters (Tcm) of technically recoverable shale gas in Europe. Taking into account that the exploitation of unconventional gas can be accompanied by serious health risks due to the release of toxic chemical components and natural occurring radionuclides into the return flow water and their near-surface accumulation in secondary precipitates, we investigated the release of U, Th and Ra from black shales by interaction with drilling fluids containing additives that are commonly employed for shale gas exploitation.

We performed leaching tests at elevated temperatures and pressures with an Alum black shale from Bornholm, Denmark and a Posidonia black shale from Lower Saxony, Germany. The Alum shale is a carbonate free black shale with pyrite and barite, containing 74.4 μg/g U. The Posidonia shales is a calcareous shale with pyrite but without detectable amounts of barite containing 3.6 μg/g U.

Pyrite oxidized during the tests forming sulfuric acid which lowered the pH on values between 2-3 of the extraction fluid from the Alum shale favoring a release of U from the Alum shale to the fluid during the short-term and in the beginning of the long-term experiments. The activity concentration of ^{238}U is as high as 23.9 mBq/ml in the fluid for those experiments. The release of U and Th into the fluid is almost independent of pressure. The amount of uranium in the European shales is similar to that of the Marcellus Shale in the United States but the daughter product of ^{238}U, the ^{226}Ra activity concentrations in the experimentally derived leachates from the European shales are quite low in comparison to that found in industrially derived flowback fluids from the Marcellus shale. This difference could mainly be due to missing Cl in the reaction fluid used in our experiments and a lower fluid to solid ratio in the industrial plays than in the experiments due to subsequent fracking and minute cracks from which Ra can easily be released.

Key words: unconventional gas production, black shales, flowback, radioactivity, NOR, batch experiments

1. Introduction

Increasing gas production from unconventional shale gas plays in the United States (U.S.) and the related engineering improvements for shale gas production in terms of drilling and hydraulic fracturing took also exploitation of European shale gas under consideration. The U.S. Energy Information Administration (U.S. EIA, 2013) estimated that Europe could hold 13.4 Tcm (trillion cubic meters) technically recoverable shale gas. A similar value of 15.9 Tcm was estimated by the European Commission's Joint Research Centre (JRC, 2012). 132 shale gas exploitation and appraisal wells have been drilled in Europe so far, most of them in Poland, Sweden and the UK (AAPG, 2016). Due to commercial viability, political barriers and public concerns, roughly 2/3 of all companies relinquished their concessions or let them expire (AAPG, 2016). In Germany, eight wells were drilled since 2008 in the Wealden or in the Posidonia formation (both Lower Saxony) but no details about the gas flow were published. One well was drilled in the Alum shale in Denmark and the drilling of 17 shallow wells into the Alum shale of Ostergötland is reported for Sweden from which only some showed a gas flow (AAPG, 2016).

The production of unconventional gas is linked with a high-pressure injection of several thousand cubic meters of water for each well (Gregory et al., 2011; SEAB, 2011) to create minute cracks in which hydrocarbons can flow to the wellbore. The formation and the operator determine the composition of the suspension for injection that is generally made of 90% water, 9 - 9.5% sand or ceramics and 1 - 0.5% chemical additives (e.g. Arthur et al., 2008; King, 2012; Wood et al., 2011). Additives could include small volumes of mainly hydrochloric acid (< 10 m^3) injected during the initial stage of the gas exploitation to clean perforation tunnels and dissolve carbonate precipitates that seal veins. Chelating agents (e.g. citric, acetic acid) are added to the fracturing fluid to prevent the precipitation of iron and manganese compounds. Additional ingredients of the fracturing fluid could be corrosion inhibitors, friction reducers, surfactants, clay stabilizers, biocides and cross-linkers tailored for the specific lithological conditions (e.g. Arthur et al., 2008; Stringfellow et al., 2014). In practice, 10 - 80% of the injected suspension returns to the surface: the so called flowback (Arthur et al., 2008; Wood et al., 2011). The amount of flowback depends on formation characteristics, well design and operating parameters.

To date, much of the research on the environmental impacts of unconventional gas production is related to the origin of gas leakages during drilling, exploitation and production (e.g. Molofsky et al., 2013), the chemical composition of the flowback (e.g. Barbot et al. 2013; Chermak and Schreiber, 2014; Dieterich et al., 2016; Gregory et al., 2011; Gordalla et al., 2013; Renock et al., 2016), the release of microbiota and organic molecules from the shales (e.g. Hölzer et al., 2016; Strong et al., 2013; Zhu et al., 2015) and the enrichment of toxic trace elements like As, Cd, Co, Cr, Hg, Ni, Zn, U, V in the flowback (e.g. Marcon, et al., 2017; Wilke et al., 2015; Chermak and Schreiber, 2014 and references therein). Some studies deal with the release of naturally occurring radionuclides (NORs) of oil- and gas-field produced waters, scales or drill cuttings but these studies cover only very specific

2

80   areas such as the Marcellus shale in the Appalachian Basin (U.S.) (e.g. Chem and Sharma, 2016; Phan

81   et al., 2015; Nelson et al., 2015 & 2014; Haluszczak et al., 2012; Rowan et al., 2011; NYSDEC,

82   2009), the Bowland shale in the UK (Environment Agency, 2011) or one shale in Pomerania, Poland

83   (Mykowska et al., 2015; Mykowska and Hupka, 2014). Therein, the focus is on alpha particle emitter

84   of the ^{238}U -, ^{235}U - and ^{232}Th - decay series e.g. ^{226}Ra (Fig.1).

85   ^{238}U series nuclides are often enriched in TOC-rich shales when U was scavenged as U(IV) under

86   reducing conditions (e.g. Chen and Sharma, 2016; Chermak and Schreiber, 2014; Schovsbo, 2002;

87   Stetten et al., 2018; Raiswell and Berner, 1985). It can be assumed that the reservoir of leachable U-

88   series nuclides initially relates dominantly to scavenging and/or chemical precipitation of uranium

89   from weathering fluids whereas the proportion of U^{238}- and Th^{232}-series nuclides re-mobilized from

90   weathering resistant minerals (e.g. zircon) is negligible. Uranium may be initially co-precipitated with

91   Fe(Mn)OOH (Muller et al., 1995 and references therein) or hosting in biogenic calcite (Russell et al.,

92   1994) and may be initially or post-depositional immobilized as U(IV) to form, e.g. secondary uraninite

93   (UO$_2$), coffeinite (U(SiO$_4$)$_{1-x}$(OH)$_{4x}$) or autunite (Ca[(UO$_2$)(PO$_4$)]$_2$ · 10 - 12 H$_2$O), depending on the

94   composition of the coexisting fluids during early stages of sediment burial (Duff et al., 2002;

95   Fredrickson et al., 2000; Cumberland et al., 2016; Lecomte et al., 2017).

96   The release of U into the drilling fluid may depend on the amount of leachable U available from the

97   shale deposits processed for gas exploitation but also from the carbonate and sulfide contents of the

98   shale (e.g. Nelson et al., 2015; Wilke et al., 2015). Interaction of pyrite-rich shales with oxic fluids

99   generates sulfuric acid that dissolves carbonates and can generate fluids with low pH when the

100   buffering capacity of the carbonate gets exhausted (Chermak and Schreiber, 2014; Wilke et al., 2015).

101   Decrease in pH favors the release of weakly bound cations from cation exchange sites and the

102   solubility of minerals hosting uranium. If acids are present, either as ingredient in the fracturing fluid

103   or formed by fluid-rock interactions during the course of shale gas production, U(IV) would be mobile

104   even under reducing conditions (Garrels and Christ, 1965). Oxygen-containing fluids force the

105   formation of easily soluble U(VI)-oxyanions. U(VI) or U(IV) release due to pH decrease during solid-

106   fluid interactions may be associated with the formation of less soluble secondary U(VI) or U(IV)

107   precipitates with CO$_3^{2-}$ or PO$_4^{3-}$ that may counteract uranium increase in the return fluids (Sandino &

108   Bruno, 1992; Stetten et al., 2018).

109   ^{226}Ra (T$_{1/2}$= 1600 a; ^{238}U - series) and ^{228}Ra (T$_{1/2}$=5.76 a; ^{232}Th-series) behave less mobile in natural

110   environments (e.g. Vengosh et al., 2014), though they frequently show slightly enhanced activities in

111   groundwater compared to their activities in surface waters (Schettler et al., 2015 and references

112   therein). ^{226}Ra and ^{228}Ra are preferentially sorbed to ion-exchange sites of particle surfaces (Ames et

113   al., 1983), get co-precipitated with BaSO$_4$ or BaCO$_3$ (Langmuir and Riese, 1985) or may be taken up

114   by plants (Bettencourt et al., 1988). Moreover, Ra is efficiently scavenged by Mn(IV)-hydroxides

115   which finds analytical application as a pre-concentration step for Ra (Charette et al., 2015 and

116   references therein). These reactions will lower the concentration of dissolved Ra in the drilling fluid

117 and can yield substantial accumulative enrichments of Ra and its decay products (^{210}Pb, ^{210}Po) in

118 coexisting solids at near-surface compartments (e.g. Nelson et al., 2015 and references therein).

119 In this study, we determine and assess the activity concentrations of ^{238}U, and ^{232}Th from one Alum

120 and one Posidonian black shale and, furthermore, the activity concentration of ^{238}U and the radioactive

121 decay product ^{226}Ra from the experimentally derived black shale leachates. We intend to increase the

122 knowledge about the amount of radioactive elements that might be enclosed in the drill cutting waste

123 and that may become mobilized from black shales into the fluids, the radioactivity they produce and

124 how European shales prospected for gas production differ in this topic from shales used for

125 unconventional gas production in the U.S. (e.g. the Marcellus shales).

126

127 **2. Experimental settings**

128 2.1 Black shales

129 A black shale sample from the Upper Cambrian Alum shale of Scandinavia (Skelbro-2, Bornholm,

130 Denmark) and one from the lower Jurassic Posidonia shale of central Europe (Haddessen, NW-

131 Germany) were chosen to simulate temporal changes in the composition of flow back water by

132 solid/fluid interaction in lab experiments under defined conditions (Table 1; Fig. 2; see Wilke et al.,

133 2015 for details). The selection of shales was done in accordance with a perspective shale gas

134 production (Horsfield et al., 2010). Both samples were taken from cores (not from cuttings) in

135 lithologies suitable for industrial gas production. Samples have been milled to < 2 mm grain size and

136 were not sieved to preserve different grain size fractions.

137

138 2.2 Extraction experiments

139 We designed two experimental set-ups consisting of A) 250 ml Erlenmeyer flasks connected with a

140 reflux condenser for short-term experiments (24 h) under atmospheric pressure and at 100°C and B) of

141 800 ml autoclaves made of a Ni-Cr-Mo-W alloy (Hastelloy™) coated inside with

142 polytetrafluoroethylene (PTFE), for long-term studies of 2 and 6 month at 100 bar and 100 °C. Latter

143 conditions roughly simulate the target formation in Damme 3 well (Lower Saxony, Germany), where

144 hydraulic fracturing was performed in a shale at ca. 1-1.5 km depth at a pressure of 110-150 bar and a

145 temperature of ca. 80 °C (Olsson et al., 2013). Both experimental set-ups run under oxidizing

146 conditions. A solid to liquid ratio of 1:12.5 was applied for both experimental set-ups. Fluids in the

147 autoclaves were O_2-saturated and overlaid by headspace containing 1% O_2 at the beginning of the

148 experiment and 0.2% O_2 at the end. About 3 ml fluid was sampled at each sampling time for HR-ICP-

149 MS measurements and the pH measured instantaneously before degassing to avoid a change in pH.

150 After sampling, the pressure in the autoclave was re-adjusted to 100 bar by adding N_2 from the gas

151 pressure bottle. Further experimental details are given in Wilke et al. (2015).

152

153 2.3 Analytical methods

154   We determined the initial mineralogical compositions of both shales using X-ray diffraction analysis

155   (XRD) using a PANalytical Empyrean (Table 1). Elemental concentrations in the shales were

156   determined by high resolution inductively coupled plasma mass spectrometry (HR-ICP-MS,

157   THERMO ELEMENT XR) following HF-aqua regia (1/1) digestion, fuming with $HClO_4$ and dilution

158   by 1/1000 with 2% HNO_3 (Table 2, Supplement 1). Reaction fluids from the experiments were filtered

159   using a 0.45 µm Nylon membrane filter and diluted by 1/10 with 2% HNO_3 before HR-ICP-MS

160   analyses. For all measurements, calibration solutions with concentrations of 0.25 and 10 µg/l were

161   applied and at least three aliquots of the reaction fluids were analyzed. The uncertainty for all ICP-MS

162   analyses is about 2-5%. The detection limits of the applied analytical routine using ICP-MS in the high

163   resolution mode typically ranged between 0.5 and 1 ng/g depending on the element.

164

165   2.4 Gamma-spectrometry

166   An amount of 4 ml out of 30-50 ml reaction fluid of the two short-term and on the beginning and the

167   end of both long-term experiments was used for gamma spectrometry. Special treatment was needed

168   for the reaction fluid from the short-term experiment using Alum. 40 ml fluid were diluted to 50 ml

169   with 5% HNO_3 prior analysis to dissolve precipitations from the fluid. Fluid activities were measured

170   using a high purity well-type germanium detector of Canberra (cryostat model: 7915-30-ULB). 4 ml

171   of the fluids were filled in PE tubes (d= 15 mm, h = 45 mm) for gamma measurements (Table 2).

172   Our measurements aimed on the quantification of Ra activity concentrations of the ^{238}U- and ^{232}Th-

173   decay series. The Ra release of ^{238}U and ^{232}Th-decay series into the extraction fluids could be in

174   similar order of magnitude due to Th and U concentrations of the shales.

175   Presumed ^{226}Ra equilibrium with ^{238}U, the theoretical number of counts for ^{214}Pb (^{238}U-series nuclide)

176   at 351.92 keV exceeds the sum of counts for ^{226}Ra and ^{235}U 3.5-fold. Nonetheless, we decided to

177   perform the ^{226}Ra determinations at 186 keV for the following arguments: a) Background peaks of

178   ^{214}Pb at 295.21 keV and 351.92 keV may vary over time due to changes in the ^{222}Rn concentration of

179   the lab-air b) we cannot be sure about the impermeability to ^{222}Rn of the PE-tubes used and c) the

180   efficiency calibrations that considered the ^{222}Rn distribution between the headspace and the 4 ml fluid

181   in the PE tubes were not available when we performed the measurements.

182   The 186 keV peak is affected by ^{226}Ra at 186.211 keV (3.64%) and ^{235}U at 185.715 keV (57.0%)

183   (NuDat2.7 Database (NNDC) 2017). Interferences by ^{234}Pa at 186.15 keV with a recommended

184   intensity of 0.00325 (Huang and Wang, 2011) and by ^{234m}Pa at 184.7 keV with an intensity of 0.00168

185   (NuDat2.7 Database (NNDC) 2017) are neglectable. Detector calibration based on the measurement of

186   a dilution of 4 ml NIST4966 Standard (289.1 Bq/ml) in the PE tube (41071 counts, uncertainty 0.53%,

187   t_{meas}= 1919 s) yielded an efficiency of 0.49 at 186 keV. The inferred detector efficiency might be an

188   overestimation if the standard includes impurities of ^{235}U. An efficiency calibration using solid powder

189   of Nussloch loess which considered ^{235}U interference corrections for assumed ^{238}U-^{226}Ra equilibrium

190   with the same fill height in the PE tube (IAG reference material data sheet) yielded a detector

191 efficiency of 0.47 at 186 keV that supports the plausibility of the efficiency calibration for the 4 ml

192 fluid aliquots.

193 Uncertainty values for γ-counting at 186 keV of the fluid samples from the lab experiments varied

194 between 5.4 and 16.8% (Table 2). Calculations followed the equations given in Supplement 2.

195 Corrections for interferences by ^{235}U are based on ^{238}U concentration measurements using ICP-MS

196 (Table 2). We considered an $^{238}U/^{235}U$ ratio of 137.818 ± 0.045 (Hiess et al., 2012) which corresponds

197 to an activity ratio of 21.709.

198 Long-term background measurements did not yield significant photopeaks at 186 keV above the

199 background scatter. We did not consider spectral coincidences for photopeak measurements at 186

200 keV which are minor (e.g. Yücel et al., 2010). A slight photopeak at 351.92 keV of ^{214}Pb (35.6%)

201 (t_{meas}= 13 days, 153 counts, uncertainty 26.4%) mostly represents the ^{222}Rn activity in the measuring

202 room and is not related to a significant ^{226}Ra blank of the detector. Otherwise, it would be related to a

203 ^{226}Ra activity blank concentration of 0.3 mBq/ml.

204 The ^{232}Th-decay series includes ^{224}Ra and ^{228}Ra. The most intense photopeak of ^{224}Ra at 240.98 keV

205 (4.1%) was not strong enough to be measurable in the extraction fluids of our experiment. Less intense

206 photopeaks of ^{228}Ra occur in the low-energy range, outside of our measuring span. Alternatively, the

207 short-lived ^{212}Pb of the ^{224}Ra decay is detectable by its strong photopeak at 238.62 keV (43.6%) which

208 is inferred by ^{224}Ra at 240.98 keV (4.1%). We only obtained a photopeak at 238.62keV (t_{meas}=

209 1208830 s, 235 counts) in the fluid sampled at the beginning of the long-term experiment using Alum

210 Shale.

211

212 **3. Results**

213 3.1 Shales

214 The XRD data show significant differences in mineralogy between the Alum shale from Bornholm,

215 Denmark and from the Posidonia shale from Lower Saxony, Germany (Table 1). The Alum shale is

216 non-calcareous and contains high amounts of pyrite whereas the Posidonia shale is carbonate rich and

217 contains a lower amount of pyrite. ICP-MS data show a more than 20-times higher U content in the

218 Alum shale (74.4 µg/g) compared to the Posidonia shale (3.6 µg/g; Table 2). 11.1 µg/g of ^{232}Th was

219 obtained from the Alum shale and 6.6 µg/g from the Posidonia shale.

220

221 3.2 Fluids

222 Due to pyrite oxidation and the formation of sulfuric acid during the course of the experiment the pH

223 in the reaction fluid of the Alum shale declined to 2-3 (Table 2, Suppl. Table 1, Fig. 3), whereas the

224 reaction fluid in contact with the Posidonia shale increased up to 7-8. Under oxidizing but neutral

225 conditions during the short-term experiment with the carbonate-rich Posidonia shale ca. 0.2% of the

226 uranium was mobilized from the shale (Table 2, Fig. 3). Under oxidizing and acidic conditions during

227 the short-term and at the beginning of the long-term experiments using the pyrite-rich Alum shale and

228   EF ca. 32% and 22% of the uranium was mobilized, respectively (Fig. 3). ^{232}Th was released from the

229   Alum shale to the fluid with ca. 22% at the beginning of the long-term experiments and with ca. 0.8 %

230   during the short-term experiment using the Alum shale and EF (Table 2, Fig. 3).

231   The activity concentration of ^{238}U is as high as 23.9 mBq/ml in the fluids of the short-term experiment

232   with the Alum shale. During the long-term experiment with the Alum shale ^{238}U-activity

233   concentrations, calculated on the basis of the ICP-MS analyses, decreased from 16 mBq/ml to 0.0006

234   mBq/ml. For all Posidonia shale extracts the activity concentration of ^{238}U is very low ($\leq$ 0.0075

235   mBq/ml) or below detection limit. The activity concentrations for ^{226}Ra lie between 3.5 and

236   5.0 mBq/ml in Alum shale experiments (Table 2). The activity concentrations of dissolved ^{226}Ra

237   remained unchanged at 4.1 mBq/ml between the beginning and the end of the long-term experiment

238   with the Posidonia shale using the extraction fluid (EF).

239

240   **4. Discussion**

241   A study of the International Atomic Energy Agency (IAEA, 2003), which compiles the current

242   knowledge about the characteristics, occurrence in various compartments, and activity concentration

243   ranges of natural radionuclides at oil and gas exploitation sites (Chapter 5.3; page 55 and Chapter 5.5;

244   page 56), states that ^{238}U and ^{232}Th are not mobilized and largely remain in the reservoir (IAEA, 2003).

245   The U content of the Alum shale from Denmark used in our experiments (74.4 µg/g) is a little lower

246   than the mean values of the two upper Cambrian Alum shales in Bornholm, namely from the Olenus

247   and Peltura zones with 92 µg/g and 100 µg/g, respectively, and is similar to the lower-most

248   Ordovician Alum shale from Denmark with 73 µg/g (Schovsbo, 2002) and an Alum black shale from

249   Sweden (72.6 µg/g; Lavergren et al., 2009). It is shown that the primary enrichment of U in the upper

250   Cambrian Alum shale has likely been taken place by the diffusion of ions through the seafloor along

251   sulfate reductions horizons at or above the sediment-water interface (Schovsbo, 2002). During the

252   middle Cambrian, scavenging of uranium onto organic particles lead primarily to the uranium

253   enrichment in the Alum shales (Lecomte et al., 2017). The Posidonia shale contains 3.6 µg/g U.

254   Comparing both European shales with the Marcellus shale in the U.S., the investigated shales show

255   comparable contents in U whereas the experimentally derived leachates show a much lower ^{226}Ra

256   activity (Table 2) than published Ra activities of the flowback water from the Marcellus shale. The

257   Devonian Marcellus shale is known for particularly high U contents compared to those of other shales

258   in the U.S., such as Eagle Ford, Utica or Antrim (Chermak and Schreiber, 2014; Kargbo et al., 2010).

259   Whole rock ICP-MS analyses show 13.5±0.3 µg/g U for a Marcellus shale from the Chenago County,

260   NY (Renock et al., 2016), between 0.6 and 72.3 µg/g U for a Marcellus shale from Greene County, PA

261   (Chen and Sharma, 2016) and 2-47 µg/g for Marcellus shale from the Tioga and Greene Counties, NY

262   and PA respectively (Phan et al., 2015).

263　In our experiment, the non-calcareous U-rich Alum shale behaves differently than the calcareous

264　Posidonia shale. The reaction fluid of the calcareous Posidonia shale had a pH of 7-8 during the course

265　of the experiments and only 0.2% of the U was mobilized from the solids. The pyrite-rich and

266　carbonate-free Alum shale leads to an acid reaction fluid with a pH of 2-3 containing max. 32% of the

267　U that the shale initially contained (Fig. 3). One has to take into account that the Alum shale has no

268　carbonate that could counteract the pH decrease in the fluid due to oxidizing of pyrite. The actual

269　uranium concentrations in the shale and the substantially higher pyrite concentrations in the Alum

270　shale compared to the Posidonia shale are the driving prerequisites to generate the high U-content in

271　the extraction fluids. ^{238}U is detectable for all extracts except for the beginning of the long-term

272　experiment using the Posidonia shale. We obtained enhanced ^{238}U activities, calculated on the basis of

273　the ICP-MS analyses, in the reaction fluids during the short-term (23.9 mBq/ml) and at the beginning

274　of the long-term (16.0 mBq/ml) experiment using the Alum shale.

275　Compiled Marcellus shale flowback data show a max ^{238}U activity concentration of 5.6 mBq/ml with a

276　median (N=16) of 0.012 mBq/ml but there is no information about the sampling time after hydraulic

277　fracturing (e.g. Abualfaraj et al., 2014; Haluszczak et al. 2012 and references therein). Following

278　hydraulic fracturing, an increase in the U concentration of the produced water was observed during the

279　first week in the Marcellus shale (Phan et al., 2015) and in the Niobrara formation, NE-Colorado

280　(Rosenblum et al., 2017) whereas in later stages of the gas exploitation the U concentration dropped.

281　This is similar to the results of our long-term experiment using the Alum shale (Fig. 3). After U(IV) is

282　oxidized to the soluble and hence readily mobile U(VI) it could scavenged by FeOOH precipitates or

283　reduced again inorganically by Fe^{2+} or Mn^{2+} species (via e.g. $Fe^{2+}\Leftrightarrow Fe^{3+}+e^-$) that are either present

284　dissolved in the aqueous phase or structurally sorbed to phyllosilicates, phosphates or oxides (e.g.

285　Stetten et al., 2018 and references therein). Oxidation of pyrite, present in the Marcellus, Alum and

286　Posidonia shales (Table 1) yields reactive Fe^{2+} that was leached in our experiments.

287　Due to their age, the ^{226}Ra activity concentrations of both shales leached in our experiments can be

288　assumed to be in secular equilibrium with ^{238}U. The ^{226}Ra activities of the low-pH Alum shale extracts

289　slightly exceeded those of the Posidonia shale (Table 2) in the long-term experiments. Obtained ^{226}Ra

290　activity concentrations from the Alum shale extracts seem to increase during the course of that

291　experiment but are similar taken the given count uncertainties into account. Therefore, our findings do

292　neither support nor oppose results of produced waters from the Marcellus shale by Rowen et al. 2011

293　in which the total Ra activities have been found to be higher in later production stages.

294　A rough Ra release estimation from the shales into the extraction fluids, taken into account the U

295　concentration of the solids determined by ICP-MS, the ratio of solids and liquids used during the

296　experiments and the presupposed equilibrium between ^{238}U and ^{226}Ra show that ca. 80% of the solid-

297　bound ^{226}Ra was released from the Posidonia shale but only <5% from the Alum shale. We suggest

that the detectable minor percentages of Ra released from the Alum shale into the fluid could point to co-precipitation of Ra with secondary sulfates (Fisher, 1998) like moorhousite and bianchite that were evident using X-ray diffraction (see Wilke et al., 2015 for details) or to a recrystallisation of barite (Grandia et al., 2008). The Ba concentrations in the Posidonia extractions increased during the course of the long-term experiment, whereas the increase of dissolved sulphate associated with the oxidation of pyrite for the Alum shale experiment might have counteracted a Ba increase in the coexisting fluid by the precipitation of Ba-rich sulfates (Supplement 1).

Ra can be remobilized from particle surfaces by replacement with other similar cations such as Ca, depending on their concentration in the extraction fluid and/or released by dissolution of chemical precipitates. Radiation damage may favor Ra liberation from solids but is unlikely. Secondary precipitates of U less strongly bind ^{226}Ra than detrital minerals such as zircons that also host ^{232}Th. At the beginning of the short-term experiment using Alum shale we measured weak ^{224}Ra and ^{212}Pb photopeaks, indicating very low ^{228}Ra activity concentrations. The dominance of ^{226}Ra versus ^{228}Ra in the experimental fluids is likely related to differences in the solid substrates hosting ^{238}U and ^{232}Th. ^{226}Ra-bearing solids may be dominantly represented by chemical precipitates hosting U from which ^{226}Ra is easily released, whereas ^{228}Ra should be predominantly hosted in fluvial or aeolian debris that more strongly embeds the ^{232}Th-series nuclides. Substantial ^{226}Ra/^{228}Ra fractionation associated with precipitation from the fluid or due to cation exchange is unlikely.

The Pennsylvania Department of Environmental Protection (PA DEP, 2009; unpublished) analyzed 25 flowback fluids from Devonian Marcellus shale typically using gamma-spectrometry and obtained a ^{226}Ra activity concentration as high as 625 mBq/ml (median A[^{226}Ra]: 22 mBq/ml; max. total (^{226}Ra+^{228}Ra): 667 mBq/ml; median total (^{226}Ra+^{228}Ra): 35 mBq/ml). The New York State Departments of Environmental Conservation (NYSDEC, 2009) detected a ^{226}Ra activity concentration as high as 593 mBq/ml out of 13 flowback fluids (median A[^{226}Ra]: 203.1 mBq/ml) from the Marcellus shale. Since there is no information about the analytical method, the data need to be handled with care (Nelson et al., 2014). Latter study observed 670±26 mBq/ml in Marcellus shale flowback water. The United States Geological Survey (USGS) analyzed 14 production waters from Devonian Marcellus shale in Bradford County, PA and obtained a ^{226}Ra activity concentration as high as 201 mBq/ml (median A[^{226}Ra]: 64 mBq/ml; max. total (^{226}Ra+^{228}Ra): 231 mBq/ml; median total (^{226}Ra+^{228}Ra): 91 mBq/ml Rowen et al., 2011). Here, Ra was co-precipitated with Ba and the precipitate measured by gamma-spectrometry. All studies revealed median activities that are higher than the industrial effluent discharge limit of 2.2 mBq/ml for ^{226}Ra (U.S. Nuclear Regulatory Commission, 2011).

For comparison, the Environment Agency of UK published a report in 2011 about the Bowland shale. The flowback of the Preese Hall well showed ^{226}Ra activity concentrations between 14±2.1 and 90±12

mBq/ml. This is three to twenty-times higher to our experimental findings of 3.5 - 5.0 mBq/ml using the Alum shale but in the range of median ^{226}Ra activities for Marcellus shale flowback fluids derived by PA DEP (2009) and Rowen et al. (2011). In a recent publication from Jodłowski et al. (2017), returned frackturing fluids, drilling mud and proppants as well as drill cuttings were subject to activity measurements from multiple rigs from either the Baltic basin or the Lublin Trough in north-eastern Poland. The returned fracturing fluids were sampled after a set a solid–fluid separators on-site. The ^{238}U activity concentrations (< 30 mBq/ml) and the ^{226}Ra activity concentrations (2-70 mBq/ml; median 43 mBq/ml) of the Polish sites cover our experimental data.

In contrast to the U concentration in flowback fluids at shale gas production sites, the activity concentration of Ra was found to be higher in late stage production waters of active industrial shale gas production (e.g. Haluszczak et al., 2012) but kept quite constant in both long-term experiments. The main reason for elevated Ra activities in flowback fluids from production sites compared to those from our reaction fluids could be seen in the fluid itself because our experimental fluids do not have elevated Cl concentrations (e.g. Kraemer and Reid, 1984; Fisher, 1998; Vengosh et al., 2014; Nelson et al., 2015) and our experiments do not simulate connected intra-and intergranular pores filled with reservoir water (Dresel and Rose, 2010) from which Ra can easily release. Furthermore, a smaller fluid to solid ratio due to minute cracks in grains after subsequent hydraulic fracturing in industrial drills would also explain the differences in the activity concentrations of ^{226}Ra.

5. Conclusions

The Posidonia shale from Germany and the Alum shale from Denmark, both differ in their mineralogical and chemical composition were chosen to quantify the release of U, Th and Ra by solid/water interaction in long-term lab experiments under defined experimental conditions. Temperature, pressure, and initial fluid composition roughly simulated the target formation in Damme 3 well, Lower Saxony, Germany. The flow through character regarding the solid/fluid interaction, however, could not be simulated in the static lab experiments, which probably underestimated the solid/fluid ratio during the real gas exploitation. The release of U into the extraction fluid appears to be independent from pressure and independent from the pH of the initially applied fluid during gas exploitation (Wilke et al., 2015) but depends on the carbonate and sulfide contents of the shales and therewith also from the pH of the resulting fluid as well as the amount of leachable U in the shale. Our findings point to a preferential Ra release from U-hosting solids.

The carbonate-rich Posidonia shale which contains less U and Th than the non-calcareous and pyrite-rich Alum shale also releases comparably low amounts of U and Th whereas the Ra release from the shales into the extraction fluid was similar. Both European shales show comparable contents in U than reported by the USGS for the Marcellus shale. However, the experimentally derived flowback samples show much lower Ra activity concentrations than the flowbacks from the Marcellus shale. The main reasons could be a) the missing Cl in our reaction fluid that is naturally present in the reservoir fluids,

369 b) that in industrial plays the fluid to solid ratio is most probably smaller c) minute cracks and well

370 connected intra-and intergranular pore spaces facilitate the release of Ra in industrial drills and d) co-

371 precipitation of Ra or recrystallization of barite.

372

381

382 **References**

383 1. AAPG Report (American Association of Petroleum Geologists), 2016. Shale gas and shale
384   liquids plays in Europe. Prepared for AAPG Energy Minerals Division by Ken Chew.
385 2. Abualfaraj, N., Gurian, P.L., Olson, M.S., 2014. Characterization of Marcellus Shale
386   Flowback Water. Environmental Engineering Science, 31, 514-524.
387 3. Ames, L. L., McGarrah, J. E., Walker, B. A., 1983. Sorption of trace constituents from
388   aqueous solutions onto secondary minerals. II. Radium. Clays and Clay Minerals, 31, 335-
389   342.
390 4. Arthur, J.D., Bohm, B., Layne, M., 2008. Hydraulic fracturing considerations for natural gas
391   wells of the Marcellus shale. The Ground water protection council 2008 Annual Forum,
392   Cincinnati, Ohio.
393 5. Bettencourt, A. O., Teixeira, M. M., Elias, M. D., Faisca, M. C., 1988. Soil to plant transfer of
394   radium-226. Journal of Environmental radioactivity, 6, 49-60.
395 6. Barbot, E., Vidic, N. S., Gregory, K. B., Vidic, R. D., 2013. Spatial and temporal correlation
396   of water quality parameters of produced waters from Devonian-age shale following hydraulic
397   fracturing. Environmental science & technology, 47, 2562-2569.
398 7. BGR, 2016. Schieferöl und Schiefergas in Deutschland. Potentiale und Umweltaspekte. BGR,
399   Federal Institute for Geosciences and Natural Resources, Hannover: 197 pp.
400 8. Buchardt, B., Nielsen, A.T., Schovsbo, N.H., 1997. Alun Skiferen I Skandinavien. Geologisk
401   Tidskift,3, 1-30.
402 9. Charette, M. A., Morris, P. J., Henderson, P. B., Moore, W. S., 2015. Radium isotope
403   distributions during the US GEOTRACES North Atlantic cruises. Marine Chemistry, 177,
404   184-195.
405 10. Chen, R., Sharma, S., 2016. Role of alternating redox conditions in the formation of organic-
406   rich interval in the Middle Devonian Marcellus Shale, Appalachian Basin, USA.
407   Palaeogeography, Palaeoclimatology, Palaeoecology, 446, 85-97.
408 11. Chermak, J. A., Schreiber, M. E., 2014. Mineralogy and trace element geochemistry of gas
409   shales in the United States: Environmental implications. International Journal of Coal
410   Geology, 126, 32-44.
411 12. Cumberland, S. A., Douglas, G., Grice, K., Moreau, J. W., 2016. Uranium mobility in organic
412   matter-rich sediments: A review of geological and geochemical processes. Earth-Science
413   Reviews, 159, 160-185.
414 13. Dieterich, M., Kutchko, B., Goodman, A., 2016. Characterization of Marcellus Shale and
415   Huntersville chert before and after exposure to hydraulic fracturing fluid via feature relocation
416   using field-emission scanning electron microscopy. Fuel, 182, 227-235.

14. Dresel, P. E., Rose, A. W., 2010. Chemistry and origin of oil and gas well brines in western Pennsylvania. Open-File Report OFOG, 10 (01.00).

15. Duff, M. C., Coughlin, J. U., Hunter, D. B., 2002. Uranium co-precipitation with iron oxide minerals. Geochimica et Cosmochimica Acta, 66, 3533-3547.

16. Environment Agency UK, 2011. Shale gas north west–monitoring of flow back water.

17. European Commission's Joint Research Centre, Energy Security Unit, 2012. Unconventional gas: Potential energy market impacts in the European union. DOI 10.2790/52499.

18. Fisher, R. S., 1998. Geologic and geochemical controls on naturally occurring radioactive materials (NORM) in produced water from oil, gas, and geothermal operations. Environmental Geosciences, 5, 139-150.

19. Fredrickson, J. K., Zachara, J. M., Kennedy, D. W., Duff, M. C., Gorby, Y. A., Shu-mei, W. L., Krupka, K. M., 2000. Reduction of U (VI) in goethite (α-FeOOH) suspensions by a dissimilatory metal-reducing bacterium. Geochimica et Cosmochimica Acta, 64, 3085-3098.

20. Garrels, R. M., Christ, C. L. 1965. Solutions, minerals, and equilibria. Harper & Row, New York.

21. Grandia, F., Merino, J., Bruno, J., 2008. Assessment of the radium-barium co-precipitation and its potential influence on the solubility of Ra in the near-field. SKB Technical Report TR-08-07. Stockholm, Sweden.

22. Gregory, K.B., Vidic, R.D., Dzombak, D.A., 2011. Water management challenges associated with the production of shale gas by hydraulic fracturing. Elements, 7, 181-186.

23. Gordalla, B. C., Ewers, U., Frimmel, F. H., 2013. Hydraulic fracturing: a toxicological threat for groundwater and drinking-water? Environmental earth sciences, 70, 3875-3893.

24. Haluszczak, L. O., Rose, A. W., Kump, L. R., 2012. Geochemical evaluation of flowback brine from Marcellus gas wells in Pennsylvania, USA. Applied Geochemistry, 28, 55-61.

25. Hölzer, K., Sumner, A. J., Karatum, O., Nelson, R. K., Drollette, B. D., O'Connor, M. P., D'Ambro, E.L., Getzinger, G.J., Ferguson, P.L., Reddy, C.M., Elsner, M., Plata, D.L., 2016. Indications of transformation products from hydraulic fracturing additives in shale-gas wastewater. Environmental Science & Technology, 50, 8036-8048.

26. Hiess, J., Condon, D.J., McLean, N., Noble, S.R., 2012. ^{238}U/^{235}U systematics in terrestrial U-bearing minerals. Science, 335, 1610-1614.

27. Horsfield, B., Schulz, H. M., Aplin, A., Doornenbal, H., Moretti, I., Lorant, F., Thomas, R., 2010. Shale gas research: the way forward for Europe. Oilfield Technology, 3, 14-18.

28. Huang, X., Wang, B., 2011. Available: http://www.nucleide.org/DDEP_WG/Nuclides/Pa-234_com.pdf

29. IAEA, 2003. Radiation protection and the management of radioactive waste in the oil and gas industry. Safety reports series no.34.

30. IAG (International Association of Geoanalysts), 2017. Available: http://iageo.com/wp-content/uploads/2017/11/UoK-RM-information-sheet-26Feb2017.pdf

31. Jodłowski, P., Macuda, J., Nowak, J., & Dinh, C. N., 2017. Radioactivity in wastes generated from shale gas exploration and production–North-Eastern Poland. Journal of Environmental Radioactivity, 175, 34-38.

32. Kargbo, D.M., Wilhelm, R.G., Campbell, D.J., 2010. Natural gas plays in the Marcellus shale: challenges and potential opportunities. Environmental Science and Technology, 44, 5679-5684.

33. King, G.E., 2012. Hydraulic fracturing 101: What every representative, environmentalist, regulator, reporter, investor, university researcher, neighbor and engineer should know about estimating frac risk and improving frac performance in unconventional gas and oil wells. SPE Hydraulic Fracturing Technology Conference. Society of Petroleum Engineers.

34. Kraemer, T. F., & Reid, D. F.,1984. The occurrence and behavior of radium in saline formation water of the U.S. Gulf Coast region. Chemical Geology, 46, 153-174.

35. Langmuir, D., Riese, A. C., 1985. The thermodynamic properties of radium. Geochimica et Cosmochimica Acta, 49, 1593-1601.

36. Lavergren, U., Åström, M.E., Bergbäck, B., Holmström, H., 2009. Mobility of trace elements in black shale assessed by leaching tests and sequential chemical extraction. Geochemistry: Exploration, Environment, Analysis, 9, 71-79.

37. Lecomte, A., Cathelineau, M., Michels, R., Peiffert, C., Brouand, M., 2017. Uranium mineralization in the Alum Shale Formation (Sweden): Evolution of a U-rich marine black shale from sedimentation to metamorphism. Ore Geology Reviews, 88, 71-98.

38. Marcon, V., Joseph, C., Carter, K. E., Hedges, S. W., Lopano, C. L., Guthrie, G. D., Hakala, J. A., 2017. Experimental insights into geochemical changes in hydraulically fractured Marcellus Shale. Applied Geochemistry, 76, 36-50.

39. Muller, J. P., Manceau, A., Calas, G., Allard, T., Ildefonse, P., Hazemann, J. L., 1995. Crystal chemistry of kaolinite and Fe-Mn oxides: relation with formation conditions of low temperature systems. American Journal of Science, 295, 1115-1155.

40. Mykowska, A., Hupka, J., 2014. Radionuclides activity and effective doses referred to geological formations. Journal of Industrial and Intelligent Information Vol. 2.

41. Mykowska, A., Rogala, A., Kallas, A., Karczewski, J., Hupka, J., 2015. Radioactivity of drilling cuttings from shale resources of the lower paleozoic Baltic Basin. Physicochemical Problems of Mineral Processing, 51, 521-533.

42. Nelson, A. W., May, D., Knight, A. W., Eitrheim, E. S., Mehrhoff, M., Shannon, R., Litman, R., Schultz, M. K., 2014. Matrix complications in the determination of radium levels in hydraulic fracturing flowback water from Marcellus Shale. Environmental Science & Technology Letters, 1(3), 204-208.

43. Nelson, A. W., Eitrheim, E. S., Knight, A. W., May, D., Mehrhoff, M. A., Shannon, R., Litman, R., Burnett, W.C., Forbes, T.Z., Schultz, M. K., 2015. Understanding the radioactive ingrowth and decay of naturally occurring radioactive materials in the environment: an analysis of produced fluids from the Marcellus Shale. Environmental health perspectives, 123(7), 689.

44. NNDC (National Nuclear Data Center), 2017. NuDat version 2.7 Database. Available: http://www.nndc.bnl.gov/nudat2/.

45. NYSDEC (New York State Department of Environmental Conservation), 2009. Draft supplemental generic environmental impact statement (SGEIS) on the oil, gas, and solution mining regulatory program (September 2009). Well permit issuance for horizontal drilling and high-volume hydraulic fracturing to develop Marcellus Shale and other low-permeability gas reservoirs: New York State Department of Environmental Conservation, Division of mineral resources, Bureau of oil and gas regulation, appendix 13.

46. Olsson, O., Weichgrebe, D., Rosenwinkel, K. H., 2013. Hydraulic fracturing wastewater in Germany: composition, treatment, concerns. Environmental earth sciences, 70, 3895-3906.

47. Phan, T. T., Capo, R. C., Stewart, B. W., Graney, J. R., Johnson, J. D., Sharma, S., Toro, J., 2015. Trace metal distribution and mobility in drill cuttings and produced waters from Marcellus Shale gas extraction: Uranium, arsenic, barium. Applied Geochemistry, 60, 89-103.

48. Raiswell, R., Berner, R. A., 1985. Pyrite formation in euxinic and semi-euxinic sediments. American Journal of Science, 285, 710-724.

49. Rosenblum, J., Nelson, A. W., Ruyle, B., Schultz, M. K., Ryan, J. N., Linden, K. G., 2017. Temporal characterization of flowback and produced water quality from a hydraulically fractured oil and gas well. Science of the Total Environment, 596, 369-377.

50. Schettler, G., Oberhänsli, H., Hahne, K., 2015. Ra-226 and Rn-222 in saline water compartments of the Aral Sea region. Applied Geochemistry, 58, 106-122.

51. Schovsbo, N.H., 2002. Uranium enrichment shorewards in black shales: A case study from the Scandinavian Alum Shale. GFF, 124, 107-115.

52. SEAB, 2011. The SEAB Shale Gas Production Subcommittee. Ninety-Day Report.

53. Stetten, L., Mangeret, A., Brest, J., Seder-Colomina, M., Le Pape, P., Ikogou, M., Zeyen, N., Thouvenot, A., Julien, A., Alcalde, G., Reyss, J. L. Bombled, B., Rabouille, C., Olivi, L., Proux, O., Cazala, C., Morin, G., 2018. Geochemical control on the reduction of U (VI) to mononuclear U (IV) species in lacustrine sediments. Geochimica et Cosmochimica Acta, *222*, 171-186.

54. Stringfellow, W.T., Domen, J.K., Camarillo, M.K., Sandelin, W.L., Borglin, S., 2014. Physical, chemical, and Biological characteristics of compounds used in hydraulic fracturing. Journal of hazardous materials, 275, 37-54.

55. Strong, L. C. Gould, T., Kasinkas, L., Sadowsky, M.J., Aksan, A., Wackett, L.P., 2013. Biodegradation in waters from hydraulic fracturing: Chemistry, microbiology and engineering. Journal of Environmental Engineering.

56. Renock, D., Landis, J. D., Sharma, M., 2016. Reductive weathering of black shale and release of barium during hydraulic fracturing. Applied Geochemistry, 65, 73-86.

57. Rowan, E.L., Engle, M.A., Kirby, C.S., Kraemer, T.F., 2011. Radium Content of oil- and gas-field produced waters in the northern Appalachian Basin (USA): Summary and Discussion of Data. US Geological survey scientific investigations report 5135.

58. Russell, A. D., Emerson, S., Nelson, B. K., Erez, J., & Lea, D. W., 1994. Uranium in foraminiferal calcite as a recorder of seawater uranium concentrations. Geochimica et Cosmochimica Acta, 58, 671-681.

59. U.S. Energy Information Administration (EIA), 2013. Technically Recoverable shale oil and shale gas resources: an assessment of 137shale formations in 41countries outside the United States.

60. U.S. Nuclear Regulatory Commission, 2011. Internet: http://www.nrc.gov/reading-rm/doc-collections/cfr/part020/appb/Radium-226.html

61. Vengosh, A., Jackson, R. B., Warner, N., Darrah, T. H., Kondash, A., 2014. A critical review of the risks to water resources from unconventional shale gas development and hydraulic fracturing in the United States. Environmental Science & Technology, 48, 8334-8348.

62. Whitney, D. L., Evans, B. W., 2010. Abbreviations for names of rock-forming minerals. American mineralogist, 95, 185-187.

63. Wilke, F. D., Vásquez, M., Wiersberg, T., Naumann, R., Erzinger, J., 2012. On the interaction of pure and impure supercritical CO 2 with rock forming minerals in saline aquifers: An experimental geochemical approach. Applied Geochemistry, 27, 1615-1622.

64. Wilke, F. D., Vieth-Hillebrand, A., Naumann, R., Erzinger, J., Horsfield, B., 2015. Induced mobility of inorganic and organic solutes from black shales using water extraction: Implications for shale gas exploitation. Applied Geochemistry, 63, 158-168.

65. Wood, R., Gilbert, P., Sharmina, M., Anderson, K., 2011. Shale gas: a provisional assessment of climate change and environmental impacts. The Tyndall Centre Manchester.

66. Yücel., H., Solmaz, A.N., Köse, E., Bor, D., 2010. A semi-empirical method for calculation of true coincidence corrections for the case of a close-in detection in gamma-ray spectrometry. Journal of Radioanalytical and Nuclear Chemistry, 283, 305-312.

67. Zhu, Y., Vieth-Hillebrand, A., Wilke, F. D., Horsfield, B., 2015. Characterization of water-soluble organic compounds released from black shales and coals. International Journal of Coal Geology, 150, 265-275.

Figure Captions

Fig. 1 Upper radioactive decay chains for A) ^{238}U and B) ^{232}Th. Half-lives are given: a=years, d=days, h=hours, m=minutes, s=seconds. Half-lives from the international nuclear structure and decay data network under the auspices of the IAEA. https://www-nds.iaea.org/relnsd/NdsEnsdf/QueryForm.html. Radionuclides marked by a green background were quantitatively determined for this study.

Fig. 2 Geographic map showing the location of described black shales in Europe. The map was adapted from the Esri World Geocoder. The Alum shale distribution is modified from Buchardt et al., 1997 and the Posidonia shale distribution adapted from the BGR (2016). Red circles show our sample locations.

Fig. 3 ICP-MS analyses of U and Th of fluids sampled during the course of long-term experiments using both shales and the extraction fluid (EF). The uncertainty is approx. 5%. On the secondary axis, the pH is given.

A) Uranium-238

Uranium	^{238}U 4.47x10^9 a	^{234}U 2.45 x10^5 a
Protactinium	^{234m}Pa 6.7h / ^{234}Pa 1.2 min	99.81% / 0.19%
Thorium	^{234}Th 24.1 d	^{230}Th 7.54x10^4 a
Radium		^{226}Ra 1600 a
Radon		^{222}Rn 3.82 d

EXPLANATION

↓ Alpha decay

↗ Beta decay

B) Thorium-232

Thorium	^{232}Th 1.4 x10^{10} a	^{228}Th 1.91 a
Actinium		^{228}Ac 6.25 h
Radium	^{228}Ra 5.75a	^{224}Ra 3.63 d
Radon		^{220}Rn 55.6 s
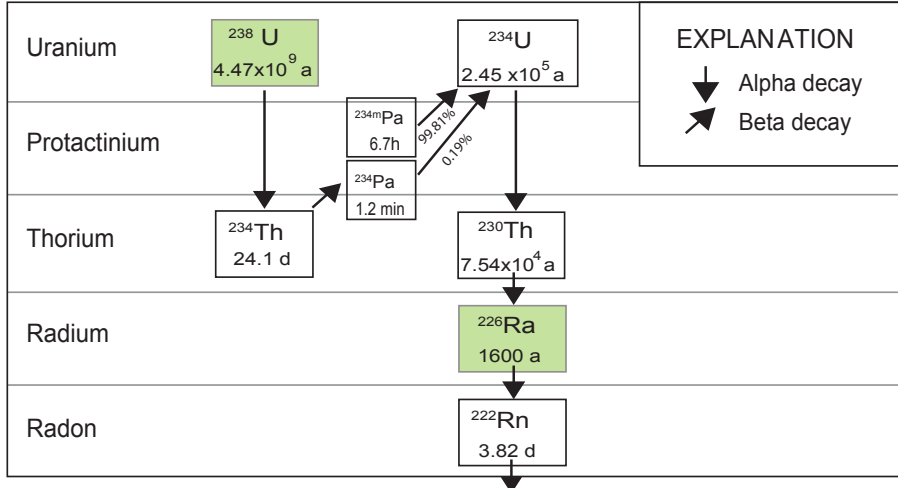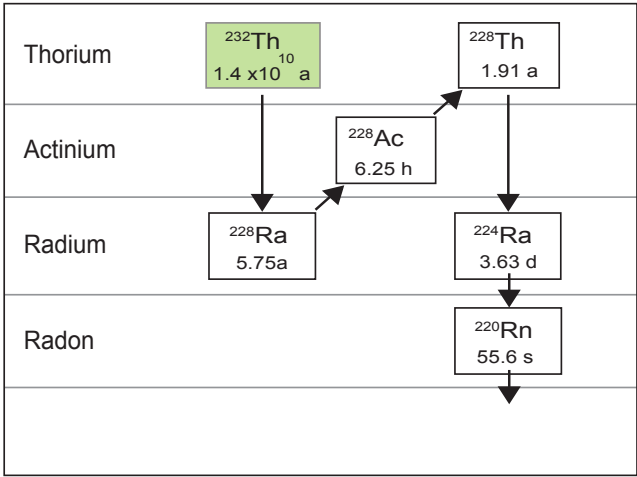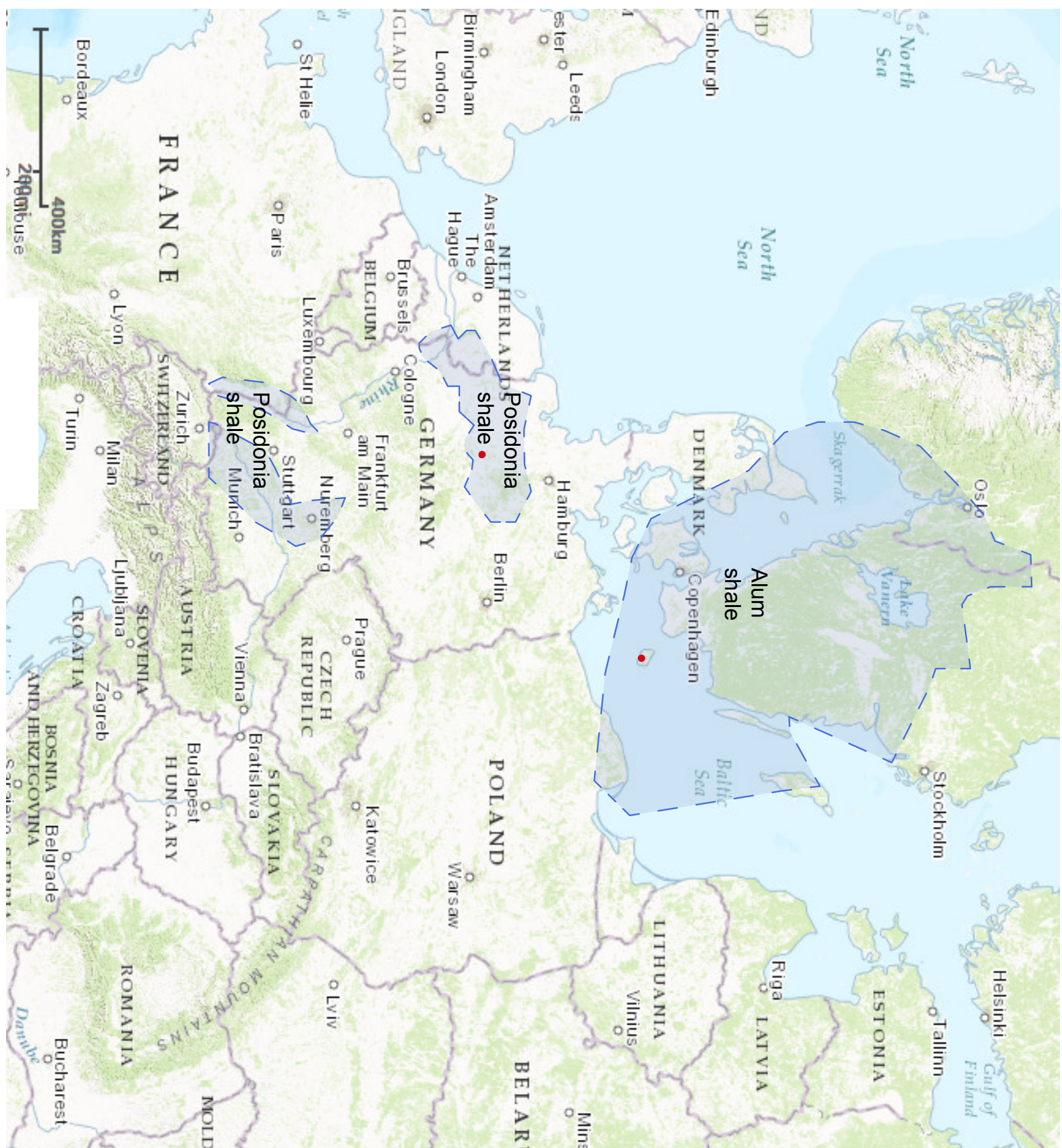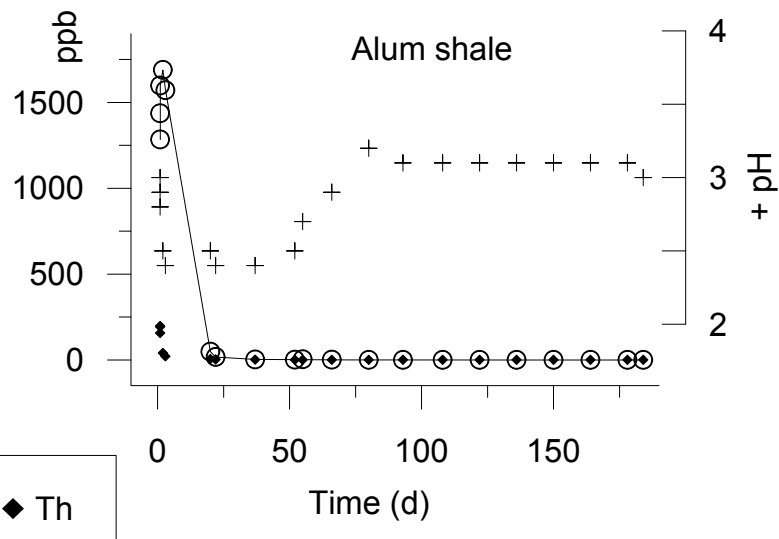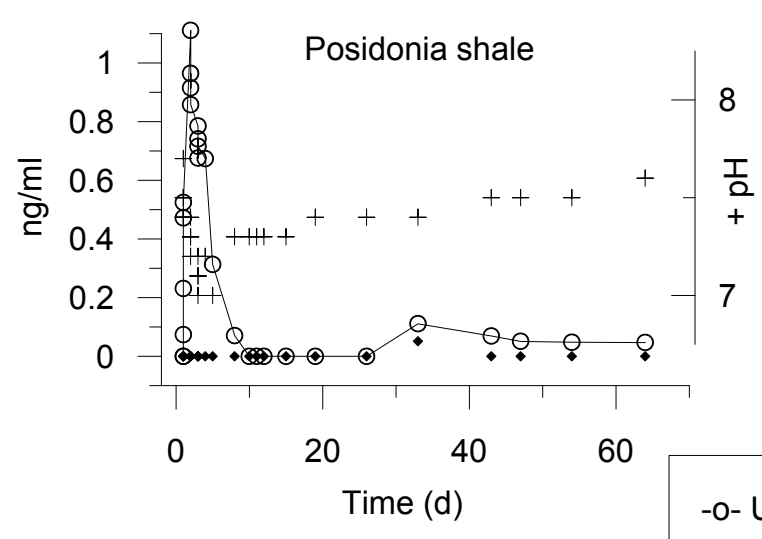
Table 1. Description and composition of black shales from europe and the US for comparison. Mineral abbreviations after Whitney and Evans, 2010.

Reference	Name	Location	Stratigraphy	Age	Depth [m]	Minerals [decresing amount]	TOC
Wilke et al., 2015	Alum 18	Bornholm (DK)	Alum shale	Upper Cambrian	18.2	Ms/Ilt, Qz, Py, Or, Brt	9.0
	Posidonien 103	Haddessen (D)	Posidonia shale	Lower Jurassic	50.8	Cb, Qz, Ms/Ilt, Kln, Py, Ab	5.6
Renock et al., 2016		Chenago County			571	Qz, Ilt, Chl, Cb, Py, Brt	-
Chen and Sharma, 2016, Marcon et al., 2017		Whipkey State#1 Greene County	Marcellus Shale	Middle Devonian	2375-2406	Qz, Cb, Ms/Ilt, Py	5.2-5.7
Phan et al., 2015		G1-G8, Greene County			2374-2407		1.0-79.7
		T1-T7, Tioga County			901-1434		1.1-52.4

Table 2. ^{232}Th and ^{238}U concentrations of shales used for leaching experiments and data for coexisting fluid compositions during the experiments. See text and supplement 2 for specifications of the radiometric analyses and for further calculation details. #) ^{238}U concentration value considered for ^{238}U-activity concentration calculations, see Supplement 1. ^{226}Ra is not in equilibrium to ^{238}U in the fluids. bdl: below detection limit. ° Values below detection limit and therefore less confidential but applied because it's statistical difference from the blank.

REACTION EDUCTS

	Solids		Extraction fluid (EF)				
	Posidonia 103	Alum 18	deionized water	biocide	surfactant	friction reducer	clay stabilizer
pH in experiment			7.0		5.9		
HR-ICP-MS ^{232}Th (µg/ml)	6.6	11.1	bdl	bdl	bdl	bdl	bdl
HR-ICP-MS ^{238}U (µg/ml)	3.6	74.4	bdl	bdl	bdl	bdl	0.001

REACTION PRODUCTS — Fluids

	Short-term experiments: **100°C/1bar** with oxygen (24 hours)				Long-term experiments: **100°C/100bar** with oxygen			
	deionized water		EF		2 month		6 month	
	Posidonia 103	Alum 18	Posidonia 103	Alum 18	Posidonia 103 Day1	Posidonia 103 Day64	Alum 18 Day1	Alum 18 Day184
amount of shale used in experiment [g]	5	5	5	5	64	64	64	64
pH in experiment	7.6	2.6	7.6	2.2	7.7	7.6	3.0	3.0
HR-ICP-MS ^{232}Th (µg/ml)	bdl	0.0005°	0.0001°	0.007	bdl	bdl	0.197	bdl
HR-ICP-MS ^{238}U (µg/ml)	bdl	0.549	0.001	1.917	bdl	bdl	1.283	bdl
^{238}U[ICP-MS] (ng/ml)#	0.6°		bdl	1917		0.05°	1283	0.05°
A[^{238}U] (mBq/ml)	0.01		bdl	23.9		6.2x10-4	16.0	5.1x10-4
Gamma-spectrometry — Δt_{meas} (s)	4087195		2998680	607731		1208830	1644805	1209169
Counts (186 keV)	1236		879	718		1358	485	427
Uncertainty (%)	9.7		12.9	7.4		5.4	16.0	16.8
A[^{226}Ra] (mBq/ml)	4.2		4.1	3.5		4.2	4.1	5.0
A[^{235}U] (mBq/ml)	3.48x10-4		2.80x10-5	1.1		bdl	0.74	2.37x10-5

Supplementary Table 1

Solids [ng/g]

	Alum	Posidonia
pH		
Li	25128	
Ni	347533	54746
Cu	154367	191
Zn	145745	91472
Rb	136698	6903
Sr	500867	69155
Y	136638	
Mo	24300	24473
Cd	190623	
Sb	4129	848
Ba	7268	748
La	17452011	190
	114000	
Tl	7765	1297
Pb	13133	9297
Th	111146	69115
U	74440	3569
V	1043432	762
Cr	113673	127
Mn	77000	71680
Fe	251558	3568
Co	50776815	57867939
As	148225	1092
	114000	27000
Ca	2759164	116628765

Reaction Fluids [ng/g] short-term experiment with EF

	Alum	Posidonia
pH	2.2	7.9
Li	59	42
Ni	13232	41
Cu	191	20
Zn	6903	6
Rb	161	24
Sr	399	4642
Y	437	804
Mo	506	1
Cd	190	
Sb	10	1
Ba	56	49
La		<1
Tl	42	1
Pb	7	<1
Th		<1
U	1917	<1
V	762	<1
Cr	127	<1
Mn	3568	95
Fe	782279	0
Co	1092	2
As	1743	<1
Ca	80911	189156

Reaction Fluids [ng/g] — long-term experiment using Alum shale and extraction fluid (EF)

day	1	1	1	2	3	20	22	37	52	55	66	80	93	108	122	136	150	164	178	184
pH	3.0	2.9	2.8	2.5	2.4	2.5	2.4	2.4	2.5	2.7	2.9	3.2	3.1	3.1	3.1	3.1	3.1	3.1	3.1	3.0
Li	50	60	72	113	150	214	229	263	271	263	262	217	227	233	241	249	231	231	229	
Ni	13127	15123	17007	19516	10931	11370	9904	9915	10776	13573	21872	13573	11740	11838	12191	13130	12083	12083	11988	
Cu	2032	1880	434	115	35	35	25	<1	<1	134	25	68	5	5	4	<1	<1	<1	<1	
Zn	6691	7728	8884	10032	9803	10286	10545	10555	9696	5855	7254	5021	5855	4310	3689	3352	616	590	585	
Rb	26	45	129	275	398	501	536	611	620	657	586	579	590	600	600	616	591	591	591	
Sr	185	231	286	480	475	145	24	26	24	12	14	16	19	22	21	22	22	22	22	
Y	277	404	531	583	179	569	521	485	441	265	189	147	129	112	101	85	86	82	82	
Mo	591	716	1033	1266	154	184	74	52	52	41	20	11	12	13	12	11	11	11	11	
Cd	183	237	264	154	145	156	65	42	40	2	1	1	1	<1	<1	14	14	11	11	
Sb	211	264	178	156	196	2	84	11	11	72	75	7	20	128	13	<1	<1	<1	<1	
Ba	3	12	21	2	52	30	44	44	2	8	31	<1	40	<1	<1	72	39	24	43	
La	35	18	12	3	12	<1	<1	<1	406	964	<1	72	<1	48	<1	<1	<1	<1	<1	
	32	42	62	46	510		1													
Tl	7	11	71	97	95	110	101	97	102	74	53	60	60	58	54	55	52	52	53	
Pb	7	14	29	2	5	3	1	1	1	1	1	14	5	14	5	1	4	4	4	
Th	197	193	156	41	20	1	1	<1	<1	1	<1	<1	<1	<1	<1	<1	<1	<1	<1	
U	1283	1437	1598	1689	1571	399	44	44	4220	1079	9	621	477	457	566	2027	363	300	285	
V	577	681	800	1105	1153	69	38	1	122	7512	8	<1	5	5	5	11	4	4	4	
Cr	338	409	477	912	764	249	249	543	5246	7162	1079	<1	<1	<1	<1	<1	<1	<1	<1	
Mn	3165	3728	4299	5092	5193	5765	5814	5246	4220	7512	7162	7169	7296	7455	7589	7069	7074	7069	7069	
Fe	704958	904177	1170817	1641740	1808846	1926009	1948600	1953576	1865044	2164341	527909	527909	524114	526838	531834	531948	516713	506359	506559	
Co	1220	1413	1662	2437	4839	4872	9674	14439	15143	13964	16309	16309	13964	14425	14801	15058	15170	15182	15503	
As	1404	1503	1911	3460	3813	2258	2325	617	58	32	5	<1	<1	<1	<1	<1	<1	<1	<1	
Ca	81421	110962	218017	255037	414712	289322	295314	301528	311172	318908	295833	213612	215978	221029	220620	219025	216945	213705	212157	

long-term experiment using Posidonia shale and extraction fluid (EF)

day	1	1	1	2	2	2	2	3	3	3	3	4	5	8	10	11	12	15	19	26	33	43	47	54	64
pH	7.7	7.5	7.4	7.4	7.5	7.4	7.3	7.4	7.2	7.3	7.1	7.0	7.1	7.2	7.2	7.0	7.3	7.3	7.3	7.4	7.4	7.5	7.5	7.5	7.6
Li	1	5	8	12	16	20	44	46	49	49	55	55	63	69	73	74	77	77	78	77	91	93	96	98	94
Ni	62	518	321	370	587	537	326	218	194	157	116	96	94	126	93	45	36	31	29	24	23	20	20	20	16
Cu	10	13	19	26	29	33	16	13	13	13	7	5	11	5	4	4	4	5	4	2	2	1	3	2	4
Zn	2	3	3	4	16	4	4	4	7	13	16	9	5	6	5	6	6	9	4	4	2	4	1	2	1
Rb	256	457	626	806	963	1118	2321	2373	2481	2500	2744	2745	2750	2789	2907	2988	3005	3050	3057	2988	2922	2800	2800	2700	2700
Sr	4	7	13	16	31	32	33	36	36	36	36	43	47	49	50	50	57	61	50	47	61	57	58	57	55
Y	457	718	930	949	1395	1257	2500	2748	2750	2994	3050	3005	2994	2989	2907	2988	3005	3050	3057	1276	2922	2800	2800	2700	2700
Mo	221	507	718	753	<1	<1	33	34	36	36	43	47	49	50	6	16	6	6	39	13	7	1	1	1	1
Cd	1	1	1	1	1196	1189	1186	1192	1186	18	14	13	14	84	89	17	18	14	21	35	17	0	0	1	1
Sb	<1	<1	63	53	53	62	66	47	48	46	44	45	54	53	44	118	119	120	118	124	132	106	113	116	118
Ba	43	38	47	<1	<1	<1	<1	<1	<1	<1	<1	<1	<1	<1	<1	<1	<1	<1	<1	<1	<1	<1	<1	<1	<1
La	<1	<1	<1																						
Tl	3	5	7	6	5	5	3	3	2	2	2	1	1	1	1	1	6	2	5	6	6	9	2	2	2
Pb	<1	<1	<1	<1	<1	<1	<1	2	2	<1	<1	<1	<1	<1	<1	<1	<1	<1	<1	<1	<1	<1	<1	<1	<1
Th	<1	<1	<1	<1	<1	<1	<1	<1	<1	<1	<1	<1	<1	<1	<1	<1	<1	<1	<1	<1	<1	<1	<1	<1	<1
U	1	1	1	1	2	2	2	2	2	<1	<1	<1	<1	<1	<1	<1	<1	<1	<1	<1	<1	<1	<1	<1	<1
V	1	1	1	1	2	1	1	2	1	<1	<1	<1	<1	<1	<1	<1	<1	<1	<1	<1	<1	<1	<1	<1	<1
Cr	62	10	26	29	16	326	218	194	157	116	96	94	126	93	45	36	31	29	24	23	20	20	20	16	94
Fe	19	12	36	30	43	54	67	106	107	108	110	109	111	100	113	112	105	99	94	70	62	56	53	50	46
Co	5	5	7	21	13	7	16	15	7	5	21	19	22	24	10	7	5	4	3	3	3	2	2	2	2
As	2	36	38		18	26	539	646	769	908	1347	1346	1457	1472	2962	3377	3162	3783	4246	5208	4130	4038	3020	2847	2465	1767
Ca	247760	38760	52760	65760	75760	93760	198760	206760	215760	219760	245760	240760	246760	249760	253760	264760	276760	278760	276760	270760	269760	259760	258760	255760	249760

Supplement 2: Specifications of the radiometric analyses and calculation formula

Variables used

Eff (186 keV)= 0.49	Detector efficiency at 186 keV
Ab[^{235}U (185.715keV)]= 57.0%	Intensity
Ab[^{226}Ra (186.21keV)]= 3.64%	Intensity
counts (186 keV)	
Δt_{meas} (s)	Measuring time
A_v= 6.02x10^{23} mol^{-1}	Avogadro constant
^{238}U$_{meas}$ (ng/ml)	ICP-MS results
A[^{238}U]$_{calc}$ (mBq/ml)	calculated on the basis of ICP-MS analyses
T$_{1/2}$[^{238}U] = 4.47x10^9 a	Half-life ^{238}U
T$_{1/2}$[^{235}U]= 7.04x10^8 a	Half-life ^{235}U
^{238}U/^{235}U = 137.818 ± 0.045 (2σ)	after Hiess et al. (2012)
A[^{238}U]/A[^{235}U] = 21.709	Reciprocal is 0.04606
V$_{meas}$ = 4 ml	Volume aliquot for γ-measurement

$$A[^{238}U](mBq/ml) = \frac{\left(^{238}U_{[meas]}(ng/mL) \times 10^{-6} \times A_v \times \ln(2)\right)}{238 \times T_{1/2}[^{238}U] \times 365.2422 \times 24 \times 3600}$$

$$A[^{235}U](mBq/ml) = \frac{A[^{238}U]}{21.709}$$

$$A[^{226}Ra]\left(\frac{Bq}{ml}\right) = \left[\frac{counts[186keV]}{V_{meas} \times t_{meas} \times Eff[186keV]} - A[^{235}U] \times 0.57\right] \times \frac{1}{0.0364}$$